

Casimir interaction between a perfect conductor and graphene described by the Dirac model

M. Bordag,¹ I. V. Fialkovsky,^{2,4} D. M. Gitman,² and D. V. Vassilevich^{3,4}

¹*Institut für Theoretische Physik, Universität Leipzig,
Vor dem Hospitaltore 1, 04103 Leipzig, Germany*

²*Instituto de Física, Universidade de São Paulo,
Caixa Postal 66318 CEP 05314-970, São Paulo, S.P., Brazil*

³*CMCC, Universidade Federal do ABC, Santo André, S.P., Brazil*

⁴*Department of Theoretical Physics, St. Petersburg State University, St. Petersburg, Russia*

We adopt the Dirac model for graphene and calculate the Casimir interaction energy between a plane suspended graphene sample and a parallel plane perfect conductor. This is done in two ways. First, we use the Quantum Field Theory (QFT) approach and evaluate the leading order diagram in a theory with $2 + 1$ dimensional fermions interacting with $3 + 1$ dimensional photons. Next, we consider an effective theory for the electromagnetic field with matching conditions induced by quantum quasi-particles in graphene. The first approach turns out to be the leading order in the coupling constant of the second one. The Casimir interaction for this system appears to be rather weak. It exhibits a strong dependence on the mass of the quasi-particles in graphene.

PACS numbers: 12.20.Ds, 73.22.-f

Keywords: Casimir energy, graphene

I. INTRODUCTION

Graphene is a (quasi) two dimensional hexagonal lattice of carbon atoms. At present, it belongs to the most interesting materials in solid state physics in view of its exceptional properties and its potential applications in nano technology (see reviews, Refs.^{1,2}). At small separations, nearly down to contact, the interaction between a graphene sample and any solid body (dielectric, conductor or another graphene) is due to the van der Waals and, at larger separations, Casimir forces (see, e.g. Refs.^{3,4}). The latter are the subject of the present paper. We consider the same geometry as in the original Casimir effect (2 parallel planes) with one plane being graphene and the other one – ideal conductor. This setup was considered in Refs.^{5,6,7} using a hydrodynamical model for the electrons in graphene following Refs.^{8,9}. Later it became clear that this model does not describe the electronic properties specific to this novel material. Here we use a realistic and well-tested model where the quasi-particles in graphene are considered to be fermions subject to the Dirac equation which models their linear dispersion law. Details of this model can be found in Refs.^{1,10}.

The result presented below is the first calculation of the Casimir interaction of graphene made within a reasonable theoretical model. Although the hydrodynamical (plasma) model is not applicable to graphene, it works well for some other materials, and it will be used as a theoretical reference point to compare our results.

We like to mention some related works. The Casimir-like interaction between adatoms due to fermionic modes *inside* graphene was studied in Ref.¹¹. The graphene-metal interaction at separations 2–4 Å (much smaller than the Casimir distances) was investigated in Refs.¹².

Let us formulate the model. The electronic properties of graphene are well described by the above mentioned

Dirac model¹⁰. It incorporates the most essential and well-established properties of the quasi-particles' spectrum: the linearity, a very small mass gap (if any), and a characteristic propagation velocity which is 300 times smaller than the speed of light. The model deals, therefore, with light fermions in $2 + 1$ dimensions (confined to the surface of graphene) with the action

$$S_D = \int d^3x \bar{\psi} (\tilde{\gamma}^l (i\partial_l - eA_l) - m) \psi, \quad (1)$$

where $l = 0, 1, 2$. The matrices $\tilde{\gamma}^l$ are rescaled, $\tilde{\gamma}^0 \equiv \gamma^0$, $\tilde{\gamma}^{1,2} \equiv v_F \gamma^{1,2}$, $\gamma_0^2 = -(\gamma^1)^2 = -(\gamma^2)^2 = 1$. v_F is the Fermi velocity. In our units, $\hbar = c = 1$, $v_F \simeq (300)^{-1}$. The gamma matrices are taken in the form of a direct sum of two inequivalent representations (differing by an overall sign). There is an additional ('valley') degeneracy in graphene, so that we have 4 two-component spinors or 2 four-component spinors in graphene. The value of the mass gap parameter m and mechanisms of its generation are under discussion^{13,14,15,16}. The upper limit on m is about 0.1 eV, but probably is much smaller. Due to this smallness of the mass, the quasi-particles exhibit a relativistic behavior at rather small energies, which makes QFT a more adequate language to describe graphene than Quantum Mechanics. As we shall see below, the Casimir force is very sensitive to the value of m , and thus the Casimir experiments may be used to estimate it.

The propagation of photons in the ambient $3 + 1$ dimensional space is described by the Maxwell action

$$S_M = -\frac{1}{4} \int d^4x F_{\mu\nu} F^{\mu\nu}, \quad \mu, \nu = 0, 1, 2, 3. \quad (2)$$

The coupling constant is normalized according to $e^2/(4\pi) = \alpha \simeq 1/137$. The Dirac model with quantized fermionic quasi-particle excitations and classical electro-

magnetic modes describes rather well the optical properties of graphene. By construction, this model should work below the energy scale of about 1eV, but even above this limit the absorption of light by suspended layers of graphene is reproduced with a high precision¹⁷.

In the following we calculate the Casimir force between a flat suspended monolayer graphene sample and a parallel flat perfect conductor. We shall suppose that the graphene sample occupies the plane $x^3 = a > 0$, and the conductor corresponds to $x^3 = 0$.

II. QFT APPROACH

One possible way to calculate the Casimir energy in the system in question is to evaluate the effective action Γ in a quantum field theory described by the classical action $S_D + S_M$. Since the background is static (the positions of the surfaces do not depend on time), the energy density per unit area of the surfaces is $\mathcal{E} = -\Gamma/(TS)$, where, because of the translation invariance, one has to divide the effective action Γ by the (temporarily introduced) time interval T and the area of the surface S . At the leading order in the fine structure constant α we have



$$\mathcal{E}_1 = -\frac{1}{TS} \text{ (diagram) }, \quad (3)$$

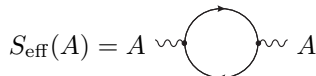
where the solid line denotes the fermion propagator in $2 + 1$ dimensions (i.e., inside the graphene sample), and the wavy line is the photon propagator in the ambient $3 + 1$ dimensional space subject to the perfect conductor boundary conditions

$$A_0|_{x^3=0} = A_1|_{x^3=0} = A_2|_{x^3=0} = \partial_3 A_3|_{x^3=0} = 0. \quad (4)$$

We use the Feynman gauge such that no contribution from ghosts appears. For details on diagrammatic notations see Ref.¹⁸.

The calculation of (3) is rather similar to that of the radiative corrections to the Casimir energy in Ref.¹⁹. The important difference to those works is that they considered the fermions propagating in the ambient space as a correction to the Casimir force between two perfect conductors, which appeared to be very small. In that case the diagram (3) represents only the $O(\alpha)$ correction to the Casimir energy. In our case, the diagram (3), still being $O(\alpha)$, represents the leading order effect.

The fermion loop in $2 + 1$ dimensions has already been calculated in a number of papers^{13,15,16}. This result is most conveniently expressed in terms of the effective action for fermions in the presence of an external electromagnetic field, $S_{\text{eff}}(A) = -i \ln \det((\tilde{\gamma}^l (i\partial_l - eA_l) - m))$. To the quadratic order in A the effective action reads



$$S_{\text{eff}}(A) = A \text{ (diagram) } A$$

$$= \frac{1}{2} \int \frac{d^3 p}{(2\pi)^3} A_j(p) \Pi^{jl}(p) A_l(p), \quad (5)$$

where

$$\Pi^{mn} = \frac{\alpha \Phi(\tilde{p})}{v_F^2} \eta_j^m \left(g^{jl} - \frac{\tilde{p}^j \tilde{p}^l}{\tilde{p}^2} \right) \eta_l^n, \quad (6)$$

$$\Phi(p) = N \frac{2m\tilde{p} - (\tilde{p}^2 + 4m^2) \text{arctanh}(\tilde{p}/2m)}{2\tilde{p}} \quad (7)$$

is the polarization tensor in the lowest, one loop, order. Here $\eta_j^m = \text{diag}(1, v_F, v_F)$, and \tilde{p} denotes the rescaled momenta $\tilde{p}_j = \eta_j^k p_k$. N is the number of two-component fermion species, $N = 4$ for graphene. Note, that in chosen above representation of gamma matrices the parity-odd parts of the polarization tensor Π are canceled between contributions of various fermion species. If they are not, due to external magnetic field or for some other reason, this may be measured by studying the polarization rotation of light passing through suspended graphene²⁰. It is also essential to notice that both polarization operator Π (6) and the diagram in (3) do not possess infra-red divergencies in the $m = 0$ limit.

To calculate the diagram (3) we only need to couple the kernel (6) to the photon propagator and integrate over the photon momenta. Symbolically,

$$\Gamma = \frac{i}{2} \text{Tr}(\Pi D), \quad (8)$$

where Tr is the functional trace, and D is the photon propagator. In the Feynman gauge the propagator $D_{\mu\nu}$ is diagonal. Since Π^{ij} by construction does not have components along the x^3 direction, we are only interested in the D_{ij} part of the propagator. According to (4), these components satisfy Dirichlet boundary conditions, and one can write

$$D_{ij}(x; y) = g_{ij}(D_0(x - y) - D_0(x - y_R)), \quad (9)$$

where $D_0(x - y)$ is the standard (Feynman) propagator of a free massless scalar field in $3 + 1$ dimensions, and the coordinate y_R is reflected at the conductor surface, $y_R^3 = -y^3$. The full effective action Γ thus reads

$$\Gamma = \frac{i}{2} \int d^3 x d^3 y \Pi_j^i(x, y) [D_0(x - y, 0) - D_0(x - y, 2a)], \quad (10)$$

where both x and y lay on the surface of graphene. After making the Fourier transform in the directions parallel to the surfaces, one can write D_0 as

$$D_0(x, y) = \int \frac{d^3 p}{(2\pi)^3} e^{ip_j(x^j - y^j)} D(p, x^3 - y^3). \quad (11)$$

For the Euclidean 3-momenta, i.e., after the Wick rotation $p \rightarrow p_E = (p_4, p_1, p_2)$, $p_4 = ip_0$, its explicit form reads

$$D(p_E, x^3 - y^3) = \frac{e^{-p_{\parallel} |x^3 - y^3|}}{2p_{\parallel}}, \quad p_{\parallel} \equiv |p_E|. \quad (12)$$

The term with $D_0(x-y, 0)$ on the right hand side of (10) does not depend on a and will be neglected (as it does not contribute to the Casimir force). The remaining terms in Γ are non-divergent. After the Fourier transformation and the Wick rotation we obtain

$$\begin{aligned}\mathcal{E}_1 &\equiv -\frac{\Gamma}{TS} = -\frac{1}{4} \int \frac{d^3 p_E}{(2\pi)^3} \frac{\Pi_j^j(p_E)}{p_{\parallel}} e^{-2ap_{\parallel}} \\ &= -\frac{1}{4} \int \frac{d^3 p_E}{(2\pi)^3} \frac{\alpha(p_{\parallel}^2 + \tilde{p}_{\parallel}^2) \Phi(p_E)}{p_{\parallel} \tilde{p}_{\parallel}^2} e^{-2ap_{\parallel}}. \quad (13)\end{aligned}$$

where we expanded $\Pi_j^j(p_E)$ explicitly with help of (6).

III. LIFSHITZ FORMULA APPROACH

One can also adopt another point of view on the Casimir effect for this system and consider an effective theory of the electromagnetic field described by the action $S_M + S_{\text{eff}}$ subject to the conductor boundary conditions (4) at $x^3 = 0$. Away from the surfaces, the photons propagate freely. They are reflected at the surface of the conductor $x^3 = 0$. At the surface of graphene, the Maxwell equations receive a singular contribution

$$\partial_{\mu} F^{\mu\nu} + \delta(x^3 - a) \Pi^{\nu\rho} A_{\rho} = 0 \quad (14)$$

following from S_{eff} . Here we extended Π to a 4×4 matrix by setting $\Pi^{3j} = \Pi^{j3} = 0$. This singular contribution is equivalent to imposing the matching conditions

$$\begin{aligned}A_{\mu}|_{x^3=a+0} &= A_{\mu}|_{x^3=a-0}, \\ (\partial_3 A_{\mu})|_{x^3=a+0} - (\partial_3 A_{\mu})|_{x^3=a-0} &= \Pi_{\mu}^{\nu} A_{\nu}|_{x^3=a}\end{aligned} \quad (15)$$

At this stage, one can forget the origin of Π_{μ}^{ν} and quantize the electromagnetic field subject to the conditions (15) at $x^3 = a$ and to the conditions (4) at $x^3 = 0$. This can be done, at least at a somewhat formal level, and even the renormalization theory can be developed, e.g. along the lines of Ref.²¹. The Casimir energy density which then are expressed through the scattering data of the electromagnetic field. There are several versions of this procedure leading to different representations for the Casimir energy – for details see Ref.³.

On the other hand, the Lifshitz approach²² relates the Casimir energy density for two parallel dielectric slabs to the corresponding dielectric permittivities taken at the imaginary frequency. In some later works^{23,24} the connection between two approaches was established and generalization of the Lifshitz formula was presented. For the interaction between two plane parallel interfaces separated by the distance a and possessing arbitrary reflection coefficients $r_{\text{TE,TM}}^{(1)}, r_{\text{TE,TM}}^{(2)}$ of the TE and TM electromagnetic modes on each of the surfaces it reads

$$\mathcal{E}_L = \int \frac{d^3 p_E}{16\pi^3} \ln[(1 - e^{-2p_{\parallel} a} r_{\text{TE}}^{(1)} r_{\text{TE}}^{(2)})(1 - e^{-2p_{\parallel} a} r_{\text{TM}}^{(1)} r_{\text{TM}}^{(2)})]. \quad (16)$$

The reflection coefficients are to be found from corresponding boundary or matching conditions. For graphene with help of (15) we obtain at the Euclidean momenta

$$r_{\text{TE}}^{(1)} = \frac{-\alpha\Phi}{2p_{\parallel} + \alpha\Phi}, \quad r_{\text{TM}}^{(1)} = \frac{\alpha p_{\parallel} \Phi}{2\tilde{p}_{\parallel}^2 + \alpha p_{\parallel} \Phi}, \quad (17)$$

while for the perfect conductor one has

$$r_{\text{TE}}^{(2)} = -1, \quad r_{\text{TM}}^{(2)} = 1. \quad (18)$$

It is clear, that Φ must be rotated to Euclidean momenta as well. We also note that the perfect conductor case is recovered from (17) in the formal limit $\Phi \rightarrow \infty$.

The Euclidean momenta representation of the Casimir energy like (16)–(18), has several advantages. First of all, it takes into account contributions from possible surface plasmon modes not requiring to analyze such modes explicitly⁶. Secondly, it is straightforward to consider its limiting cases and also perform numerical evaluations as presented in the next section.

One can show by a direct computation that the energy \mathcal{E}_1 , Eq. (13), coincides with the leading α^1 order in a perturbative expansion of the Lifshitz formula (16)–(18), so that the two approaches are consistent. In fact, the Lifshitz formula is the one-loop vacuum energy (one closed vacuum loop) in an effective theory corresponding to the action $S_M + S_{\text{eff}}$. As we have explained above, the presence of the singular part S_{eff} is equivalent to the matching conditions (15). Imposing these conditions, in turn, is equivalent to summing up the photon propagators with an arbitrary number of Π^{mn} insertions (or, with an arbitrary number of the fermion loop insertions). Therefore, the Lifshitz approach corresponds to a partial summation of diagrams of the QFT approach. We shall explain this correspondence in detail elsewhere.

IV. RESULTS AND DISCUSSION

The formulae (13) and (16)–(18) are suitable for the numerical and asymptotical evaluation. First we consider the large separation limit, $a \rightarrow \infty$. Introducing dimensionless variables $p_E \rightarrow p_E a$ in (16)–(18) we are able to expand the integrand in a power series in $1/a$. Each term of such expansion is integrable and in the leading order we get for the energy

$$\mathcal{E}_L \underset{a \rightarrow \infty}{\sim} -\frac{\alpha N}{96\pi^2} \frac{2 + v_f^2}{ma^4}. \quad (19)$$

We note that the energy is decreasing by one power of the separation a faster than for ideal conductors. Also we point out that this asymptotic expression is of the first order in the coupling constant α .

In the limit of small separation, $a \rightarrow 0$, due to the structure of the function $\Phi(p_E/a)$ the energy

$$\mathcal{E}_L \underset{a \rightarrow 0}{\sim} \frac{1}{16\pi a^3} h(\alpha, N, v_F) \quad (20)$$

factorizes into a distance dependent part and a function $h(\alpha, N, v_F)$ independent of the separation a but containing all powers of α ; in the leading order it is

$$h(\alpha, N, v_F) = -\frac{N\alpha}{16} \times \left(1 + \frac{2 + v_F^2}{\sqrt{1 - v_F^2}} \operatorname{arcsinh} \left(\frac{\sqrt{1 - v_F^2}}{v_F} \right) \right) + O(\alpha^2). \quad (21)$$

Therefore we see that the asymptotic behavior of the Casimir energy in our model shows some surprising features being drastically different from that in the hydrodynamic model^{5–7}. At large separation it does not turn into the ideal conductor case, while at small ones this case is regained. Such behavior is counter-intuitive since the main contribution at small separations shall come from the high momenta for which one would expect the graphene film to become transparent. On the other hand, the behavior at large separation results from low momentum contributions for which the Dirac model is considered to be well proved following directly from the electronic structure of graphene.

One can show that in the case of a massless (gapless) fermions the same distance dependence as for ideal conductors is retained for all distances due to lack of any dimensional parameters in this case. The magnitude of the energy is defined by the same asymptotic (20) as for the $a \rightarrow 0$ case.

Let us now turn to the numerical evaluation. It is convenient to normalize the results to the Casimir energy density

$$\mathcal{E}_C = -\frac{\pi^2}{720 a^3} \quad (22)$$

for two plane ideal conductors separated by the same distance a . The relative quantities $\mathcal{E}_1/\mathcal{E}_C$ and $\mathcal{E}_L/\mathcal{E}_C$ are dimensionless and depend on a single dimensionless parameter ma . To fix the scale, note that for $m = 0.1\text{eV}$ (actual values of m are much smaller) $ma = 1$ corresponds to $a = 1.97$ micrometer. The results of calculations are depicted at Fig. 1. For $m = 0$ the normalized energies $\mathcal{E}_{1,L}/\mathcal{E}_C$ are constant independent of a as explained above.

Thus, we can see that the magnitude of the considered Casimir interaction of graphene with a perfect conductor is rather small. Actual measurement of such weak forces is a challenging, but by no means hopeless, experimental problem³¹. Strong dependence on the mass parameter m at large separation is also a characteristic feature of the Casimir force. Getting an independent measurement of m may be very important for our understanding of the electronic properties of graphene. The mass of quasi-particles in graphene is, probably, very tiny. This improves the detectability of the Casimir interaction since the energy increases with decreasing m .

As noted above, the Casimir energy \mathcal{E}_1 calculated in the QFT approach coincides with the lowest order expansion in the coupling constant α of the Casimir energy

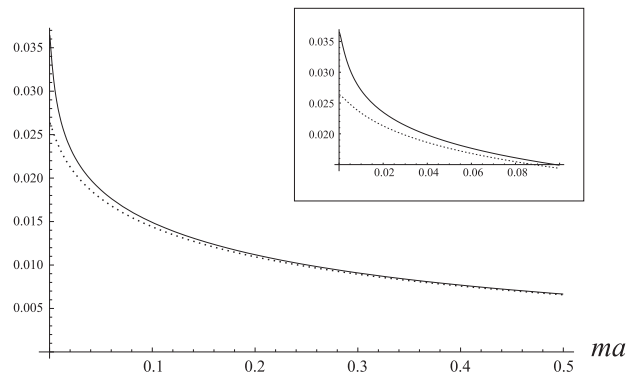


FIG. 1: The relative Casimir energy densities $\mathcal{E}_1/\mathcal{E}_C$ (solid line) and $\mathcal{E}_L/\mathcal{E}_C$ (dashed line) as functions of ma . A zoom of the small-distance region is placed in the upper-right corner.

\mathcal{E}_L derived from the Lifshitz formula. This perturbative nature of the Casimir energy in graphene systems (which is just the other side of its smallness) makes the calculations much easier and will probably simplify the analysis of other geometries like, e.g., folded or corrugated graphene near a conducting surfaces. (An example of perturbative calculations with δ -potentials with the support of a non-trivial geometry can be found in Ref.²⁵). This is in contrast with some other physical effects in graphene which exhibit a strong coupling dependence.

There are several factors that can be included in the considered model to make it more realistic. Among them the effects of non-zero temperature, corrugation of the free-standing graphene sample, presence of impurities and non-vanishing density of carriers. However, for clean enough graphene samples, similar to Ref.²⁶, all mentioned factors can be considered as perturbations not changing the essentials of the Dirac model. In particular, the corrugation was shown to maintain the massless fermionic nature of the quasi-particles²⁷, and thus can be treated perturbatively as in Ref.²⁵. The effect of impurities can also be implemented into the theory as modifications to the Dirac operator which may be considered as perturbations at least in the sense of the operator theory. Indeed, while the impurities have a significant impact on the density of states²⁸ and broaden the Landau levels in the Hall regime, their effects may be represented through adding a complex chemical potential, expressed through electronic self-energy¹⁵. Although in general the frequency dependence of these terms can significantly modify the properties of the model, in many cases the constant approximation of such broadening of Landau levels works well²⁹ and can be treated as corrections³⁰.

Thus, the method proposed above will therefore remain valid upon inclusion of these effects, and probably even numerically the corrections will remain small. Actual calculations will be the scope of our future work.

Acknowledgments

This work was supported in parts by FAPESP (I.V.F. and D.M.G.), CNPq (D.M.G. and D.V.V.), the grants RNP 2.1.1/1575 (I.V.F. and D.V.V.) and RFBR 07-01-

00692 (I.V.F.).

One of the authors (M.B.) thanks the ESF Research Network CASIMIR for providing excellent opportunities for discussion on the Casimir effect and related topics.

-
- ¹ A. K. Geim and K. S. Novoselov, *Nature Mater.* **6**, 183 (2007); M. I. Katsnelson, *Mater. Today* **10**, 20 (2007); A. K. Geim, arXiv:0906.3799 [cond-mat.mes-hall].
 - ² A. H. Castro Neto, F. Guinea, N. M. R. Peres, K. S. Novoselov, and A. K. Geim, *Rev. Mod. Phys.* **81**, 109 (2009).
 - ³ M. Bordag, G. L. Klimchitskaya, U. Mohideen, and V. M. Mostepanenko, *Advances in the Casimir effect*, (Oxford University Press, Oxford, 2009).
M. Bordag, U. Mohideen and V. M. Mostepanenko, *Phys. Rept.* **353**, 1 (2001) [arXiv:quant-ph/0106045].
 - ⁴ K. A. Milton, *The Casimir effect: Physical manifestations of zero-point energy*, (World Scientific, River Edge, 2001);
 - ⁵ G. Barton, *J. Phys.*, A38(13):2997–3019, 2005.
 - ⁶ M. Bordag, *J. Phys. A* **39**, 6173 (2006) [arXiv:hep-th/0511269].
 - ⁷ M. Bordag, B. Geyer, G. L. Klimchitskaya and V. M. Mostepanenko, *Phys. Rev. B* **74**, 205431 (2006).
 - ⁸ A. L. Fetter, *Annals of Physics*, **81**, 367, (1973).
 - ⁹ G. Barton, *J. Phys. A: Math. Gen.*, **37**, 1011, (2004).
 - ¹⁰ G. W. Semenoff, *Phys. Rev. Lett.* **53**, 2449 (1984); D. P. DiVincenzo and E. J. Mele, *Phys. Rev. B* **29**, 1685 (1984); C. L. Kane and E. J. Mele, *Phys. Rev. Lett.* **95**, 146802 (2005).
 - ¹¹ A. Shytov, D. Abanin and L. Levitov, arXiv:0812.4970 [cond-mat.mes-hall].
 - ¹² J. Wintterlin and M.-L. Bocquet, *Surface Science* **603**, 1841 (2009); D. Jiang, M.-H. Du and S. Dai, *J. Chem. Phys.* **130**, 074705 (2009).
 - ¹³ T. W. Appelquist, M. J. Bowick, D. Karabali and L. C. R. Wijewardhana, *Phys. Rev. D* **33**, 3704 (1986).
 - ¹⁴ D. V. Khveshchenko, *Phys. Rev. Lett.* **87**, 206401 (2001).
 - ¹⁵ E. V. Gorbar, V. P. Gusynin, V. A. Miransky and I. A. Shovkovy, *Phys. Rev. B* **66**, 045108 (2002) [arXiv:cond-mat/0202422]; V. P. Gusynin and S. G. Sharapov, *Phys. Rev. B* **73**, 245411 (2006) [arXiv:cond-mat/0512157]; V.P. Gusynin, S.G. Sharapov, J.P. Carbotte, *New J. Phys.* **11** (2009) 095013, [arXiv:0908.2803v2].
 - ¹⁶ P. K. Pyatkovskiy, *J. Phys.: Condens. Matter* **21**, 025506 (2009).
 - ¹⁷ R. Nair, P. Blake, A. N. Grigorenko, K. S. Novoselov, T. J. Booth, T. Stauber, N. M. R. Peres and A. K. Geim, *Science* **320**, 1308 (2008).
 - ¹⁸ P. Ramond, *Field Theory. A Modern Primer*, Front. Phys. 51:1-397, 1981.
 - ¹⁹ M. Bordag, D. Robaschik and E. Wiecezorek, *Annals Phys.* **165**, 192 (1985); D. Robaschik, K. Scharnhorst, and E. Wiecezorek, *Annals Phys.* **174**, 401 (1987); M. Bordag and J. Lindig, *Phys. Rev. D* **58**, 045003 (1998) [arXiv:hep-th/9801129]; M. Bordag and K. Scharnhorst, *Phys. Rev. Lett.* **81**, 3815 (1998) [arXiv:hep-th/9807121].
 - ²⁰ I. V. Fialkovsky and D. V. Vassilevich, *J. Phys. A: Math. Theor.* **42** (2009) 442001, arXiv:0902.2570 [hep-th].
 - ²¹ M. Bordag, I. G. Pirozhenko and V. V. Nesterenko, *J. Phys. A* **38**, 11027 (2005) [arXiv:hep-th/0508198]; D. V. Vassilevich, *Phys. Rev. D* **79**, 065016 (2009) [arXiv:0901.0337 [hep-th]].
 - ²² E. M. Lifshitz, *Zh. Eksp. Teor. Fiz.* **29**, 94 (1956) [*Sov. Phys. JETP* **2**, 73, (1956)]; E. M. Lifshitz and L. P. Pitaevskii, *Statistical Physics* (Pergamon Press, Oxford, 1980).
 - ²³ M. T. Jaekel and S. Reynaud. *Journal De Physique I*, 1(10), 1395–1409, (1991).
 - ²⁴ M. Bordag. *J. Phys.*, A28:755–766, 1995.
 - ²⁵ J. Wagner, K. A. Milton and P. Parashar, *J. Phys. Conf. Ser.* **161**, 012022 (2009) [arXiv:0811.2442 [hep-th]].
 - ²⁶ P. Neugebauer, et. al., *Phys. Rev. Lett.* **103**, 136403 (2009), [arXiv:0903.1612v2]
 - ²⁷ K. R. Knox, S. Wang, A. Morgante, D. Cvetko, A. Locatelli, T. O. Mendes, M. A. Niño, P. Kim and R. M. Osgood, Jr., *Phys. Rev. B* **78**, 201408(R) (2008)
 - ²⁸ V. M. Pereira, F. Guinea, J. M. B. Lopes dos Santos, N. M. R. Peres and A. H. Castro Neto, *Phys. Rev. Lett.* **96**, 036801 (2006) V. M. Pereira, J. M. B. Lopes dos Santos, A. H. Castro Neto, *Phys. Rev. B* **77**, 115109 (2008) Wen-Min Huang, Jian-Ming Tang, and Hsiu-Hau Lin, *Phys. Rev. B* **80**, 121404(R) (2009)
 - ²⁹ D. Shoenberg, *Magnetic Oscillations in Metals* (Cambridge University Press, Cambridge, England, 1984) R. E. Prange, *The Quantum Hall Effect*, edited by R. E. Prange and S. M. Girvin (Springer-Verlag, New York, 1987).
 - ³⁰ Thomas G. Pedersen, *Phys. Rev. B* **67**, 113106 (2003); T. Stauber, N. M. R. Peres, and A. H. Castro Neto, *Phys. Rev. B* **78**, 085418 (2008).
 - ³¹ The linear dimensions of existing suspended graphene samples reaches size of a couple of millimeters (see Geim, Ref.¹) which is well above the requirements of up-to-date Casimir experiments³. Also, the current precision of these experiments is better than fractions of a percent, which is enough to detect the Casimir interaction of graphene.